PHILOSOPHICAL TRANSACTIONS OF THE ROYAL SOCIETY A MATHEMATICAL, PHYSICAL & ENGINEERING SCIENCES

Fronts and Shelf-Circulation Models

I. D. James

Phil. Trans. R. Soc. Lond. A 1981 **302**, 597-604
doi: 10.1098/rsta.1981.0185

Phil. Trans. R. Soc. Lond. A **302**, 597–604 (1981)
Printed in Great Britain

Fronts and shelf-circulation models

By I. D. James
Institute of Oceanographic Sciences, Bidston Observatory, Birkenhead, Merseyside L43 7RA, U.K.

[Plates 1 and 2]

Satellite imagery shows that fronts and frontal eddies are widespread on the northwest European continental shelf. The implications for the numerical modelling of transports (for example, of pollutants) are discussed. A brief review of some models of shelf circulation is given. It is argued that to include fronts in models of shelf circulation requires a better understanding of dynamics on the frontal scale. A three-dimensional numerical model of eddy formation in a coastal front is then presented that reproduces many of the observed features.

1. Introduction

Numerical models of continental shelf seas designed for the study of tides and wind-driven flow have reached a level of development at which they are considered reliable enough to be used operationally in predictions of unusually high sea levels (storm surges) (Flather 1979) and the changes in the tides resulting from large constructional projects such as the proposed Severn Barrage (Owen 1979). However, models addressed specifically to the problem of the total flow on the continental shelf on longer time-scales than that of a single storm or a tidal period, which we may define as the circulation, cannot be said to have reached the same degree of reliability.

The practical motivation for circulation models is clear: it is the circulation that determines the destination of pollutants from such sources as rivers, coastal discharges or oil spills at sea, and the drift of plankton. The practical problems of measuring circulation are difficult: residual currents (that is, total currents minus the oscillatory flow due to the tides) may be measured by conventional current meters only if they are strong enough (several centimetres per second), and very many long term current meter moorings would be required to resolve the circulation pattern of an area such as the North Sea. To measure Lagrangian mean flows (these would be the paths followed by a passive pollutant moving with the water velocity) is an even greater challenge, although interesting results have been obtained by a study of radioactive discharges from nuclear power stations (Kautsky 1973; Wilson 1974; Kautsky *et al.* 1980). Therefore the testing of a circulation model against observation is much less precise than a similar test for a tidal model. In addition, more physics must be included in the model. While a two-dimensional model is perfectly adequate to predict sea level, circulation is inherently three-dimensional. Density must be included to take account of density-driven currents and other buoyancy effects: to model density *changes* involves a consideration of heat input, fresh water run-off, evaporation and precipitation. Tides and winds contribute to the circulation as well as to vertical mixing, while density stratification, if present, will tend to reduce this mixing. The parametrization of turbulent viscosity and diffusivity is still not well understood. To cover long-period motions, a numerical scheme must be designed to allow long time-steps. The spatial

resolution of the model may not have seemed a problem before the presence and the extent of fronts in shelf seas were recognized, but it is now clear that these sharp boundaries between water masses are a major feature of the continental shelf. They must have a profound effect on the circulation pattern and the transport of pollutants.

2. Satellite imagery

The most convincing, and beautiful, demonstrations of the extent of fronts have come from infrared satellite images. Here, two images are shown that illustrate some of the features that must be considered when a circulation model is contemplated. The first (figure 1, plate 1) shows the North Sea as viewed by the TIROS-N satellite on 30 September 1979 at 13h49 G.M.T. Darker tones represent higher temperatures. At this time of year, the shallow water along the coast of the Netherlands and in the German Bight has cooled below the temperature of the central North Sea, reversing the sign of the midsummer horizontal temperature gradient in these regions, and warmer water lies in a band across the North Sea from the English channel to the Skagerrak. Frontal boundaries can be seen on the northern side of this band, in the German Bight and also along the edge of the Norwegian coastal current. These do not coincide with the usual 'h/u^3' contours (fig. 6 of Pingree & Griffiths 1978) probably because that simple model does not take account of seasonal variations or fresh water input in coastal regions. Almost all the boundaries in the image show marked eddy structures. These are most striking in the entrance to the Baltic Sea, where there are complete cyclonic eddies, reminiscent of satellite pictures of depressions in the atmosphere, although in this area there appears to be some topographic control.

The eddy radius is expected to be of the order of the Rossby radius of deformation $R_d = (g'h)^{\frac{1}{2}}/f$, g' being the reduced gravity $g\Delta\rho/\rho_0$, where $\Delta\rho$ is the density difference and ρ_0 a reference density, h is the depth of the baroclinic layer and f is the Coriolis parameter (see Eady (1949) for the classical theory, Gascard (1978) for examples in the Mediterranean, and Pingree (1978, 1979) for examples on the shelf). Hence the different scales of the eddies (small in the central North Sea, larger in the German Bight and largest in the Norwegian coastal current) are a consequence of the different density contrasts and depth scales in these areas. It is interesting to note that there are small eddies on the fainter boundaries in the north central North Sea, in an area well away from the more well known fronts.

The second image (figure 2, plate 2) shows the Celtic Sea and English Channel as viewed by the NOAA-6 satellite on 16 September 1979 at 08h37 G.M.T. The fronts near the Scilly Isles and Ushant are very clear (possibly accentuated by fog). They are linked across the mouth of the English Channel, and the Ushant front is also linked to a cool band of water lying along the shelf edge (see Pingree (1979) and Dickson *et al.* (1980) for observations of this band, and Heaps (1980*a*) for a possible explanation). A further front runs along the French coast of the Bay of Biscay from the Ushant front southwards. As on the image of the North Sea, eddy structures abound, many showing a distinct cyclonic shape.

There are fainter boundaries in the central Celtic Sea complete with eddy structure, well away from the stronger fronts. So there is evidence from both images that front and associated eddy activity on various scales can be widespread throughout the shelf seas, and is not simply confined to a few well defined areas.

Eddies in both pictures resemble those produced in the laboratory by Griffiths & Linden

PHILOSOPHICAL TRANSACTIONS OF THE ROYAL SOCIETY A MATHEMATICAL, PHYSICAL & ENGINEERING SCIENCES

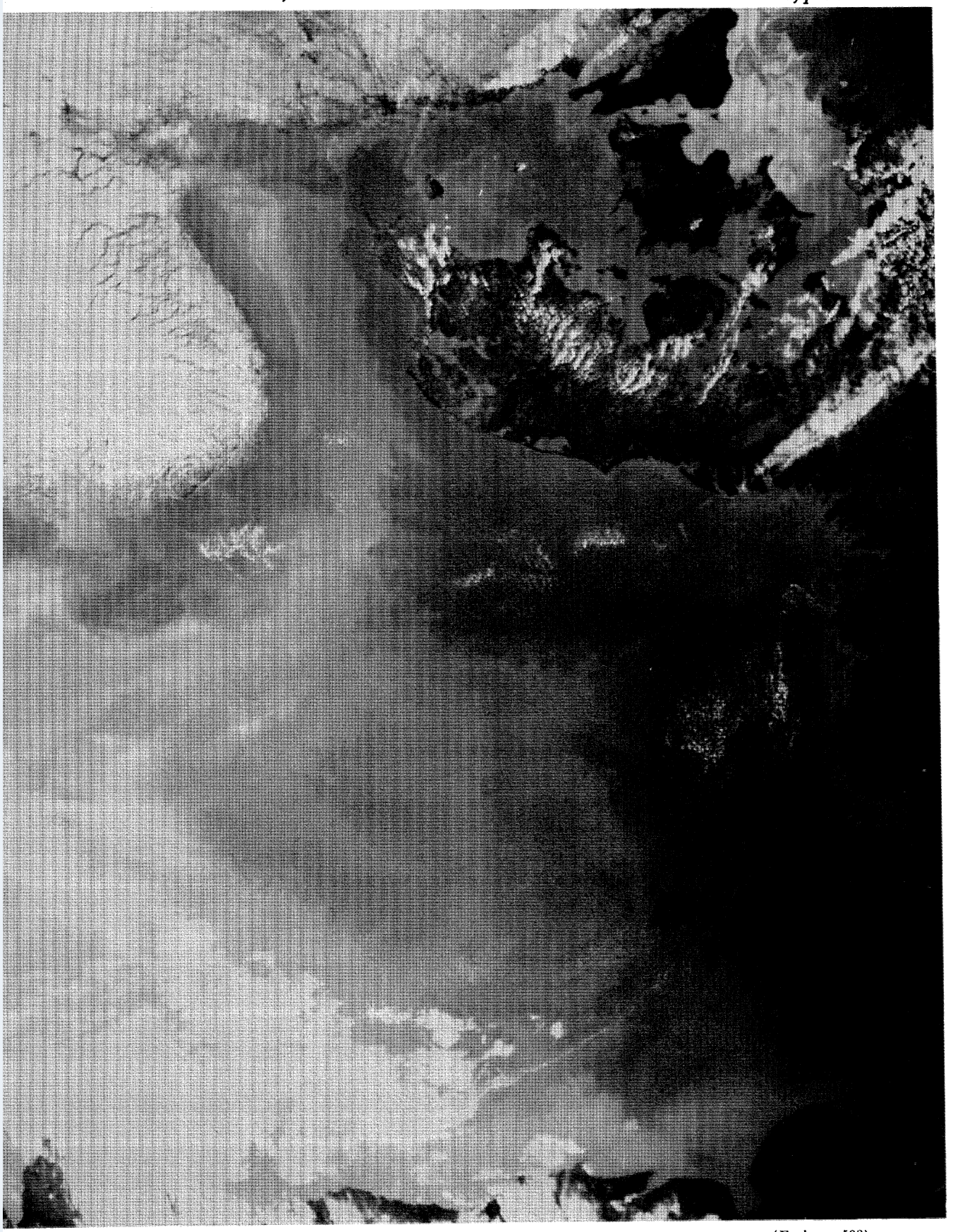

(*Facing p.* 598)

PHILOSOPHICAL TRANSACTIONS OF THE ROYAL SOCIETY A MATHEMATICAL, PHYSICAL & ENGINEERING SCIENCES

FIGURE 2. Infrared satellite image of the Celtic Sea and English Channel on 16 September 1979.

PHILOSOPHICAL TRANSACTIONS OF THE ROYAL SOCIETY A MATHEMATICAL, PHYSICAL & ENGINEERING SCIENCES

(1980). In particular, some 'hammer-head'-shaped protrusions which can be seen clearly on the Ushant front appear to match their observation of the development of vortex pairs from large-amplitude eddies, as shown in figure 3.

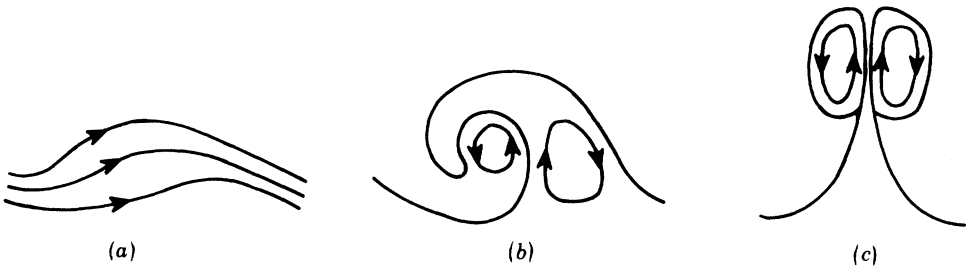

FIGURE 3. The development of a vortex pair from a large-amplitude eddy (after Griffiths & Linden 1980). (*a*) Growing wave; (*b*) developed cyclonic eddy; (*c*) vortex pair.

3. NUMERICAL CIRCULATION MODELS

Effects of fronts on the general circulation are to introduce strong residual currents in regions of small spatial extent (mostly along the front if approximate geostrophic balance can be assumed), to mark boundaries for water masses (and hence drifting material including pollutants, which may indeed become concentrated near fronts by convergent cross-frontal flow) and to control, by means of instabilities and eddy generation, the exchange of material and momentum across these boundaries. Eddies shed from fronts may affect the circulation and water mass properties at some distance from them. These effects are on a scale small compared with that of the shelf, and the fundamental problem is that of including them in a shelf-scale model. It is clear that to do this it is necessary to improve understanding of the dynamics on the frontal scale, and as a step towards this a three-dimensional model of the instability of a coastal front will be described, preceded by a brief review of some previous circulation models.

Existing models of circulation on shelves have concentrated on the study of one of the three main components of the residual flow. These are density-driven flow, wind-driven flow and tidal residuals. The density-driven flow in an area of horizontal density gradients, with application to Liverpool Bay, was modelled by Heaps (1972). This is an example of a diagnostic model, in which the given density distribution is held fixed and the steady state current deduced from the equations of motion and continuity. This model was extended to the whole of the Irish Sea by Heaps & Jones (1977) and to a two-layered system resembling the Norwegian coastal current by Heaps (1980*b*). A model similarly deriving currents from a given density structure was applied by James (1978) to a front separating stratified from well mixed water, resembling that found in the St George's Channel area of the Celtic Sea in summer. This model predicted upwelling on the well mixed side and convergence near the front as well as a strong component of flow along the front at the surface. Another form of diagnostic model was given by Hunter (1975), in which the total mean flow in the Irish Sea was deduced from the mean salinity distribution and the concentration equation for salinity on the assumptions of a horizontal diffusivity tensor dependent on tidal current, complete vertical mixing and two-dimensional flow. This, of course, does not include fronts or mixing due to frontal eddies, while many numerical models (for example, those of Heaps & Jones (1977) and Davies (1980)) do not include any horizontal eddy viscosity.

PHILOSOPHICAL TRANSACTIONS OF THE ROYAL SOCIETY A MATHEMATICAL, PHYSICAL & ENGINEERING SCIENCES

Wind-driven and tidal residuals have been calculated for the northwest European continental shelf by Davies (1981), using a three-dimensional model (described by Davies (1980)), which, by an expansion of the horizontal current components u and v in a series of continuous basis functions of the vertical coordinate z, can predict continuous vertical profiles of u and v as well as sea level, given tidal conditions on the boundary and the wind field. This model does not include any density variation. The steady wind-driven flow was calculated for three-monthly and annual mean wind fields, and reaches at the surface typically 2–10 cm s^{-1} in summer, 10–20 cm s^{-1} in winter, less (and generally in a different direction) at depth. The tidal residuals are smaller (mostly less than 3 cm s^{-1}) and are more uniform with depth. Possible effects of such flows include frontogenesis by convergent flow in an area of horizontal density gradients, while advection perpendicular to a front (into or out of a mixing region for stratified to well mixed boundaries) may influence the position and sharpness of the front. However, the success of one-dimensional models (the 'h/u^3' model of Simpson & Hunter (1974), as applied to the shelf by Pingree & Griffiths (1978), and the annual cycle model of James (1977)) in predicting the position and structure of the strongest fronts suggests that advection is a minor influence on them. It is possible that, since both fronts and, as noted by Davies (1981), residual currents (except for wind-driven currents near the surface) are linked to topography, *cross*-frontal advection is usually small.

The inclusion of stratification (and the associated variations in vertical eddy viscosity) in a model is expected to have a significant influence on the calculated wind-driven flow. Since stratified areas are usually bounded by fronts, a stratified model of shelf seas should include them in some way. The conditions to be applied at such frontal boundaries then depend on the local properties of fronts. These may be studied with the aid of small-scale models.

4. A three-dimensional front model

For models of frontogenesis in the atmosphere, the semigeostrophic equations, used by Hoskins & West (1979) to study the instability of a zonal jet, are attractive. They use the fact that momentum is approximately geostrophic in frictionless flow with small Rossby number. In shallow seas stirred by the tides, however, friction cannot be neglected: the Ekman number is not necessarily small and the Ekman layer thickness can be comparable with the water depth. The effect of friction is indeed one of the problems requiring study. The primitive equations are therefore taken here, after making the Boussinesq and hydrostatic approximations.

They are

$$\partial u/\partial t + \mathrm{L}(u) - fv = -\partial\phi/\partial x + \partial(A\,\partial u/\partial z)/\partial z \tag{1}$$

and

$$\partial v/\partial t + \mathrm{L}(v) + fu = -\partial\phi/\partial y + \partial(A\,\partial v/\partial z)/\partial z, \tag{2}$$

where $\phi = p/\rho_0$, p is the pressure deviation (total pressure $+\rho_0 gz$) and ρ_0 is a reference density. Then, if buoyancy $b = g\,(\rho_0 - \rho)/\rho_0$,

$$b = \partial\phi/\partial z \tag{3}$$

and

$$\partial b/\partial t + \mathrm{L}(b) = \partial(K\,\partial b/\partial z)/\partial z. \tag{4}$$

The parameter A is vertical eddy viscosity and K is vertical eddy diffusivity, and the operator L is given by

$$\mathrm{L}(\sigma) = \partial(u\sigma)/\partial x + \partial(v\sigma)/\partial y + \partial(w\sigma)/\partial z. \tag{5}$$

Also,

$$\partial u/\partial x + \partial v/\partial y + \partial w/\partial z = 0. \tag{6}$$

The bottom stress conditions are taken to be

$$A\,\partial u/\partial z = CVu \quad \text{and} \quad A\,\partial v/\partial z = CVv \quad \text{on} \quad z = -H, \tag{7}$$

where C is a constant (*ca.* 2.5×10^{-3}) and V is a constant velocity of the order of the tidal current.

Conditions of zero surface stress and zero buoyancy flux at surface and bottom are applied. Here, a rectangular basin is considered with periodic boundary conditions applied at the ends, and conditions of zero flux across vertical walls at the sides. The basin then becomes a section of an infinitely long channel. A 'rigid-lid' condition ($w = 0$ at $z = 0$) is applied at the surface: this removes the possibility of surface gravity waves and hence allows long time-steps.

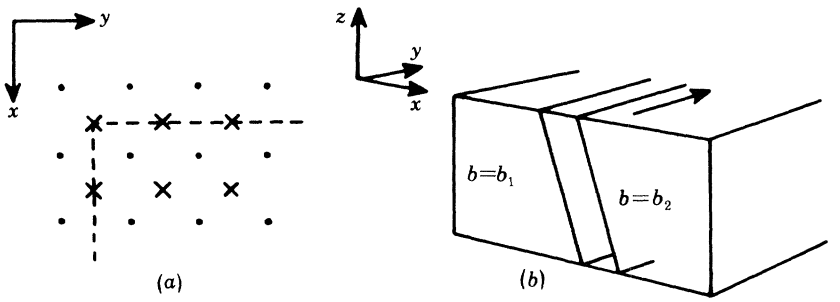

FIGURE 4. (*a*) Arrangement of grid points in the horizontal: crosses are b, ψ-points and dots u, v-points. The dashed line is the boundary of the rectangular basin. (*b*) Initial configuration for the coastal front. The buoyancy b has the values b_1 and b_2 ($> b_1$) on the two sides, separated by a sloping boundary in which b changes linearly with x from b_1 to b_2. The direction of the initial geostrophic flow is indicated by the arrow.

The method of numerical solution follows closely that of Semtner (1974), and the details will not be given here. The scheme conserves mass and energy. At each time-step, finite-difference versions of equations (1) and (2) are stepped forwards in time, surface pressure being ignored, to find the depth-dependent part of the velocity components u and v. The depth-integrated part is found by vertically averaging the finite-difference forms of (1) and (2), introducing a stream function ψ for the depth-integrated flow, and eliminating the surface pressure term from the resulting two equations. This gives a finite-difference equation for the change D in ψ over a time-step in the form $\mathscr{L}D = Q$, where $\mathscr{L}$ has the form of a finite difference Laplacian operator (generalized for the case where topography is included). Here, this equation is solved by expanding Q and D in series of trigonometric functions of one of the coordinates (the y-coordinate, along the front, in this case). The tridiagonal matrices involved in the resulting equations are the same throughout the calculation and so need to be inverted once only. In the present model the treatment of the diffusive and viscous terms used by Semtner (1974) is replaced by the Du Fort–Frankel scheme for reasons of stability, since the forward time-step scheme is highly unstable in the shallow-sea case of high friction and small grid size except for very short time-steps (it requires a time-step $\Delta t < (\Delta z)^2/2A$ for stability). The value of ψ on one side of the channel is held fixed (at zero); the value of ψ on the other side is allowed to change.

The arrangement of the grid points is shown in figure 4*a*. For the results to be presented here, a grid of 30 points in the cross-front (x) direction, 15 points in the along-front (y) direction (covering one wavelength of the perturbation to be applied) and 11 points in the vertical direction was used. The horizontal dimensions of the basic rectangle were 50 km (plus one grid interval) in the cross-front direction and 30 km in the along-front direction. The along-front

PHILOSOPHICAL TRANSACTIONS OF THE ROYAL SOCIETY A MATHEMATICAL, PHYSICAL & ENGINEERING SCIENCES

dimension was then approximately four times the calculated Rossby radius of deformation for the initial front, shown in figure 4*b*. This was taken to have dimensions and density differences typical of a coastal area (for example, the German Bight) in which there is a contrast between relatively fresh coastal water and denser, saltier water offshore. The depth was taken to be

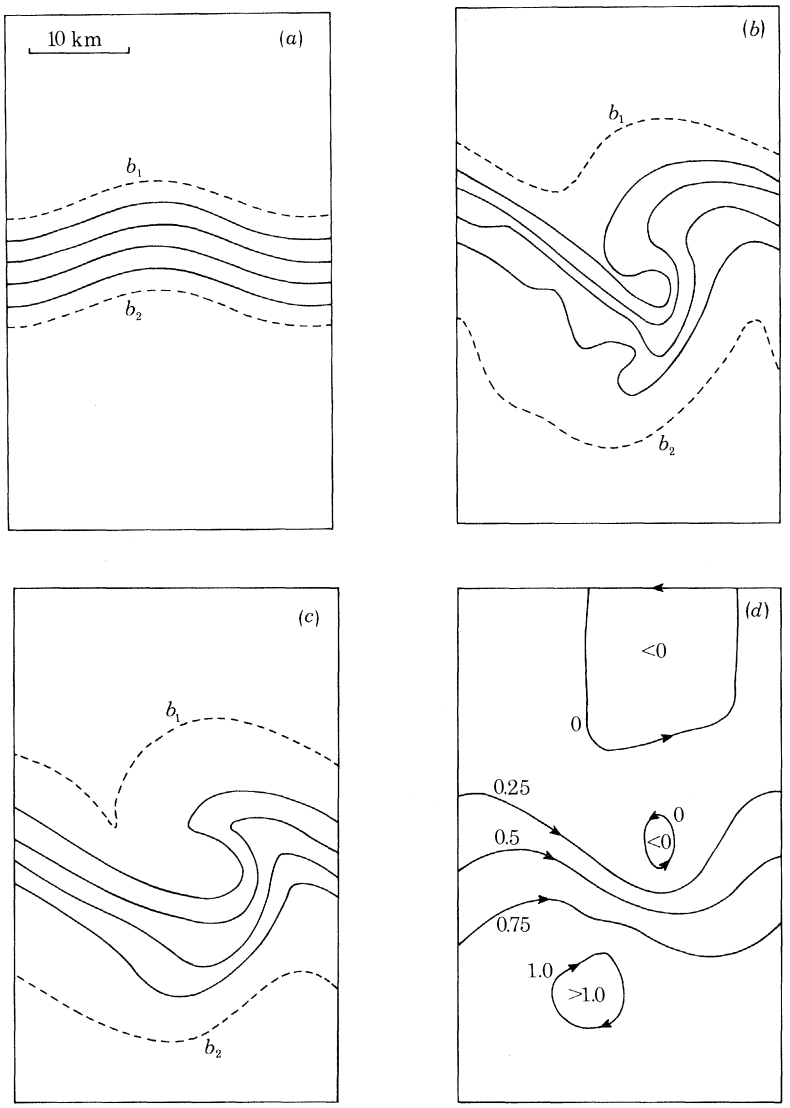

FIGURE 5. (*a*) The perturbed initial surface buoyancy field. (*b*) The buoyancy field at the surface, (*c*) the buoyancy field at the bottom, (*d*) the stream function of the depth-integrated flow (values shown are $10^{-5}\,\psi$ (m^3 s^{-1})), almost two days after the introduction of the perturbation. (In (*a*), (*b*) and (*c*) contours are equally spaced between b_1 and b_2.)

constant at 40m, σ_t was assumed to change across the front from 22 to 24, and the initial thickness of the front was 11 km. The interface slope was 1/185. The initial velocity field was taken to be the steady geostrophic velocity in the y-direction that would exist in the absence of friction, with the condition that the velocity at the bottom is zero. For simplicity, a case of constant eddy viscosity and diffusivity, with $A = K$, is taken here. Now the values of A and K in unstratified conditions are assumed to be equal to $1.59 \times 10^{-3}\,VH$ (as in James (1977), from

PHILOSOPHICAL TRANSACTIONS OF THE ROYAL SOCIETY A MATHEMATICAL, PHYSICAL & ENGINEERING SCIENCES

Bowden (1967)), but in the vicinity of the front, where there is stratification, this value is expected to be reduced. In the example given here, it is reduced to a tenth of this value, and as V is taken to be 0.5 m s^{-1} this gives reduced values of 32 cm^2 s^{-1}. It is feasible to experiment with many different formulations of eddy viscosity and diffusivity in the model, for example with values dependent on Richardson number (as in James (1977)). Further results will be given elsewhere, but it is worth noting here that with A and K equal to 320 cm^2 s^{-1} rather than the reduced value given above the flow is highly damped and eddy development is suppressed. This suggests that increased tidal mixing may actually act to *decrease* transfer across the front.

Figure 5 shows results obtained by introducing a sinusoidal perturbation of the front shown in figure 4*b*, with amplitude equal to one grid interval and wavelength equal to the along-front length of the basic rectangle (one grid interval more than this length is shown in figure 5). Figure 5*a* shows the perturbed initial surface buoyancy field. Figures 5*b*, *c* and *d* display the surface and bottom buoyancy and the stream function fields nearly two days (in fact 46.88 h) after the perturbation is introduced. These demonstrate cyclonic eddy development (with the characteristic 'backwards breaking' shape), some evidence of entrainment of the denser water in the centre of the eddy at the surface, front-sharpening (frontogenesis) behind and ahead of the eddy, along-front movement of the eddy, and a beginning of vortex pair formation (seen in the surface density field and the stream function field). Therefore the model is able to reproduce, at least qualitatively, many of the observed characteristics of frontal boundaries.

One of the implications of the model is that the strength of vertical mixing influences the ease with which eddies are developed. A variety of results for different basic density structures and eddy viscosity assumptions may be expected. The range of velocities (in both magnitude and direction) predicted in a front with eddies present may explain why a consistent measurement of geostrophic along-front flow has been difficult to achieve by current meters or drogues. The pattern of surface temperature would explain the multiple jumps, not always in the same direction, that are sometimes seen on continuous sea-surface temperature and salinity records made from a ship.

Further modelling and observational work should together help elucidate the as yet imperfectly understood processes involved in circulation in fronts. This is a necessary step towards the inclusion of the effects of fronts in shelf-circulation models.

I would like to thank Mr P. E. Baylis and his colleagues at the Department of Electrical Engineering and Electronics, University of Dundee, for supplying the satellite images.

This work was funded by the Ministry of Agriculture, Fisheries and Food.

References (James)

Bowden, K. F. 1967 *Boundary layers and turbulence. Physics Fluids* Suppl. S278–280.
Davies, A. M. 1980 *Appl. math. Modelling* **4**, 245–255.
Davies, A. M. 1981 *Oceanologica Acta.* (Submitted.)
Dickson, R. R., Gurbutt, P. A. & Pillai, V. N. 1980 *J. phys. Oceanogr.* **10**, 813–819.
Eady, E. T. 1949 *Tellus* **1**, 33–52.
Flather, R. A. 1979 *Marine forecasting* (ed. J. C. J. Nihoul), pp. 385–409. Amsterdam: Elsevier.
Gascard, J. C. 1978 *Oceanologica Acta* **1**, 315–330.
Griffiths, R. W. & Linden, P. F. 1980 In *Proc. 2nd IAHR Int. Symp. Stratified Flows*, vol. 1, pp. 81–94. Trondheim: Tapir; also 1981 *J. Fluid Mech.* **105**, 283–316.
Heaps, N. S. 1972 *Geophys. Jl. R. astr. Soc.* **30**, 415–432.
Heaps, N. S. 1980*a* *Oceanologica Acta* **3**, 449–454.

Heaps, N. S. 1980*b* *Geophys. Jl. R. astr. Soc.* **63**, 289–310.
Heaps, N. S. & Jones, J. E. 1977 *Geophys. Jl. R. astr. Soc.* **51**, 393–429.
Hoskins, B. J. & West, N. V. 1979 *J. atmos. Sci.* **36**, 1663–1680.
Hunter, J. R. 1975 *Estuar. coast. mar. Sci.* **3**, 43–55.
James, I. D. 1977 *Estuar. coast. mar. Sci.* **5**, 339–353.
James, I. D. 1978 *Estuar. coast. mar. Sci.* **7**, 197–202.
Kautsky, H. 1973 *Dt. hydrogr. Z.* **26**, 241–246.
Kautsky, H., Jefferies, D. F. & Steele, A. K. 1980 *Dt. hydrogr. Z.* **33**, 152–157.
Owen, A. 1979 *Proc. Instn. civ. Engrs* **67**, 907–928.
Pingree. R. D. 1978 *J. mar. biol. Ass. U.K.* **58**, 955–963.
Pingree, R. D. 1979 *J. mar. biol. Ass. U.K.* **59**, 689–698.
Pingree, R. D. & Griffiths, D. K. 1978 *J. geophys. Res.* **83**, 4615–4622.
Semtner, A. J. 1974 *Numerical simulation of weather and climate, tech. Rep.* **9**, Dept of Meteorology, University of California, Los Angeles.
Simpson, J. H. & Hunter, J. R. 1974 *Nature, Lond.* **250**, 404–406.
Wilson, T. R. S. 1974 *Nature, Lond.* **248**, 125–127.

PHILOSOPHICAL TRANSACTIONS OF THE ROYAL SOCIETY A MATHEMATICAL, PHYSICAL & ENGINEERING SCIENCES

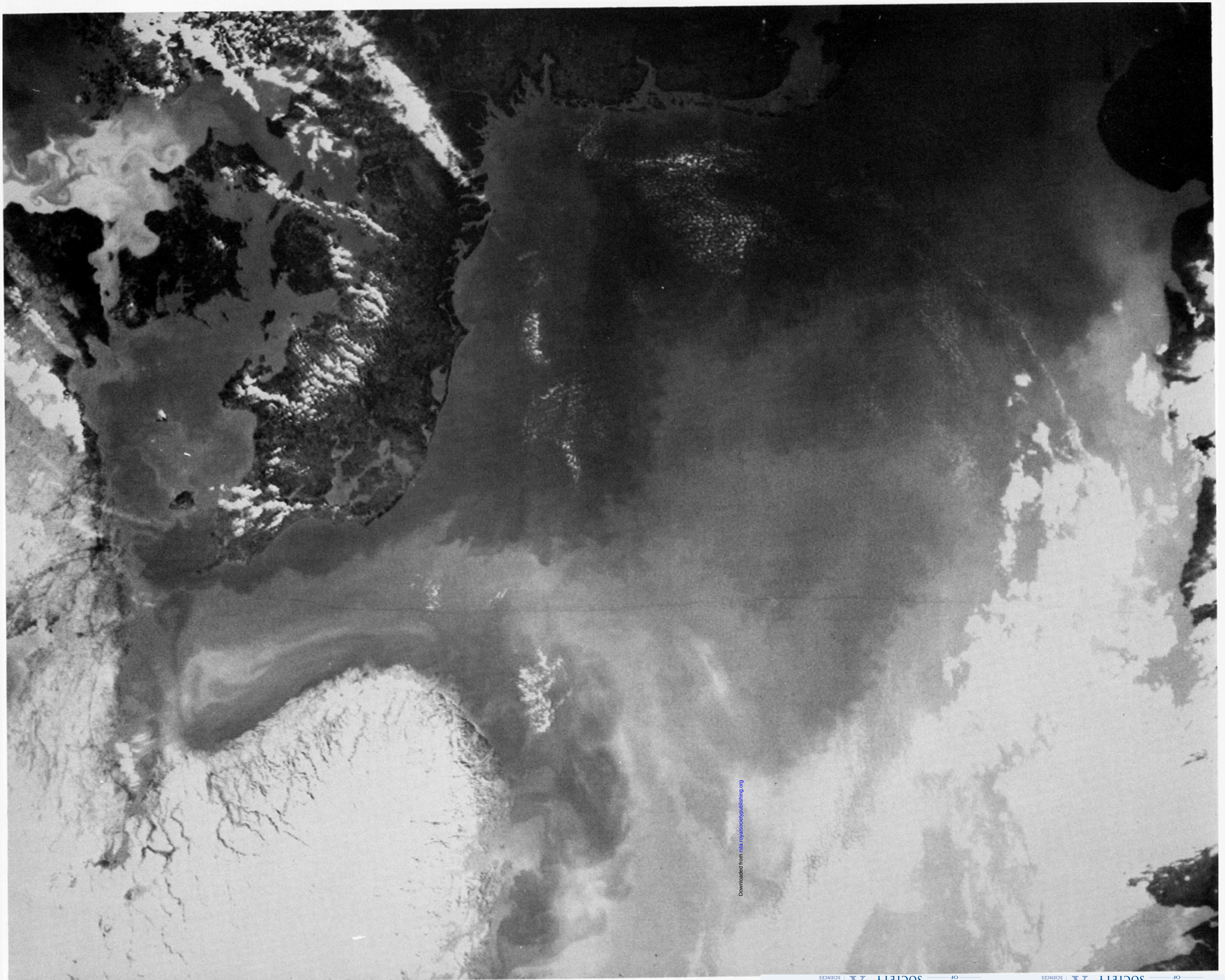

PHILOSOPHICAL TRANSACTIONS OF THE ROYAL SOCIETY A MATHEMATICAL, PHYSICAL & ENGINEERING SCIENCES

FIGURE 2. Infrared satellite image of the Celtic Sea and English Channel on 16 September 1979.